THREE-DIMENSIONAL STRUCTURE OF AN ALPHA ACCRETION DISK

Włodzimierz Kluźniak and David Kita

Physics Department, University of Wisconsin, Madison, WI 53706, USA

ABSTRACT

An analytic solution is presented to the three-dimensional problem of steady axisymmetric fluid flow through an accretion disk. The solution has been obtained through a systematic expansion in the small parameter $\epsilon = \bar{H}/\bar{R}$ (the ratio of disk thickness to its radial dimension) of the equations of viscous hydrodynamics. The equation of state was assumed to be polytropic. For all values $\alpha < 0.685$ of the viscosity parameter, we find significant backflow in the midplane of the disk occuring at all radii larger than a certain value; however, in the inner regions of the disk the fluid always flows toward the accreting object. The region of backflow is separated from the region of inflow by a surface flaring outwards from a circular locus of stagnation points situated in the midplane of the disk.

1. Introduction

Accretion flows occur in a variety of astrophysical situations, often they take the form of a disk (e.g., Frank, King & Raine 1992). The first solutions for accretion disk flows were constructed numerically by Prendergast & Burbidge (1968), while the first analytic solutions were obtained by Shakura & Sunyaev (1973). Since then, it has been the custom in analytic, but frequently also in numerical, work to discuss essentially one-dimensional solutions, i.e. to obtain the radial structure of the disk by considering equations averaged over the thickness of the disk and only then to obtain an approximate "vertical" structure by separately considering equations describing

hydrostatic equilibrium (and possibly radiation transfer) in the direction perpendicular to the plane of the disk. This is also true in discussions of quasi-spherical flows, such as in the celebrated accretion-dominated flows (ADF) (e.g Narayan 1996 and references therein)[1].

As already shown by Urpin (1984) in a remarkable paper, consideration of the vertical gradients of the stress tensor leads to a solution in which the flow direction in the midplane of the disk is opposite to that in the subsurface layers. The flow cannot be properly described by its height-averaged value, a point dramatically evident in the numerical work of Kley & Lin 1992 who enforced spurious circulation flows in the meridional plane by adopting "height-averaged" boundary conditions at the edges of their computational domain (nevertheless, they found and correctly identified an outflow in the disk midplane, reminiscent of Urpin's solution). Several recent numerical calculations (e.g. Różyczka, Bodenheimer & Bell 1994; Igumenshchev, Chen and Abramowicz 1995) also exhibit flows which can best be described in terms of a tendency for backflow to occur in the midplane of the disk. We believe this effect is not thermal in origin, and to investigate the dynamics of the phenomenon we solve analytically the three-dimensional equations of disk accretion using a polytropic equation of state for the fluid.

Urpin (1984) included thermal effects but made the simplification of zero net angular momentum flow in the disk (equivalently, his self-similar solution is valid asymptotically for large radii). In our work we chose the opposite route—we neglect

[1]In an important contribution Narayan & Yi 1995 go beyond the one-dimensional solutions by numerically constructing axisymmetric ADF solutions which factorize the three-dimensional equations, i.e., solutions of the type $f(r,\theta) = R(r)\Theta(\theta)$. However, the solutions we present in this paper are not factorizable.

thermal effects, but include the inner boundary condition—this allows us to exhibit the global character of the solution. In particular, we show how the backflow is fed by the inflowing fluid. In Section 2 we present the equations, in Section 3 we solve them. A discussion of the results is begun in Section 4 and concluded, in Section 5, with a detailed presentation of the velocity field in the disk.

1. Disk equations.

1.1. Assumptions.

We use cylindrical coordinates (r, ϕ, z) centered on the accreting object and make the following standard assumptions:

(i) the gravitational force on a fluid element is characterized by the Newtonian potential of a point mass,

$$\psi(r, z) = -\frac{GM_*}{\sqrt{r^2 + z^2}}, \tag{1.1}$$

with G the gravitational constant and M_* the mass of the central star;

(ii) the structure of the disk is symmetric under reflection about the $(z = 0)$ midplane;

(iii) the disk is in a steady state $(\partial/\partial t = 0)$;

(iv) the disk is axisymmetric $(\partial/\partial\phi = 0)$, hence all quantities will be expressed in terms of the coordinates (r, z);

(v) $|v_\phi| \gg |v_r|$;

(vi) The disk is geometrically thin, i.e. $|z| \ll r$;

(vii) Viscous torques are a small perturbation in the radial (r) and vertical (z) components of the equations of motion.

Assumption i) implies also that the disk is not self-gravitating. The assumptions iii)–v) are consistent with the statement that the accretion time scale is much greater than the Keplerian period. Assumption vi) implies that the rotational velocity is much greater than the local sound speed in the outer parts of the disk, $v_\phi \gg c_s$, and that the radial velocity is larger than the vertical one, $|v_r| \geq |v_z|$. Assumptions v)-vii) taken together signify that the disk is approximately in hydrostatic equilibrium.

Throughout this paper we will also assume that

viii) the equation of state for the disk is that of a polytrope, i.e.

$$P = K\rho^{1+1/n}, \tag{1.2}$$

with n and K constant. Except in the Appendix we will take the polytropic index to be $n = 3/2$.

For the inner boundary condition, we take vanishing of the viscous torque at some radius r_m, corresponding to a maximum of the angular frequency, Ω_m, at the same radius. This boundary condition, which introduces into the problem a natural lengthscale, $r_+ = \Omega_m^2 r_m^4/(GM_*)$, is appropriate for black-hole disks and for stellar accretion disks about stars which are spinning-up (whether magnetized or not). For stars which are not spinning up, i.e. ones which transfer their angular momentum to the disk (such as non-magnetized stars rotating close to the equatorial mass-shedding limit and, possibly, for X-ray pulsars [accreting neutron stars] in their spin-down phase), the solution presented below is valid with the substitution $1 - \sqrt{r_+/r} \to 1 + \sqrt{r_+/r}$. Thus, our solution is universally valid for any thin,

Keplerian accretion disk described by a polytropic equation of state. We expect that the qualitative features of our solution for the accretion flow will hold also for other equations of state.

If the polytropic disk were in exact hydrostatic equilibrium, the angular frequency $\Omega = v_\phi/r$ would be constant on cylinders and it would be very easy to solve the equations of motion, at least far from the inner boundary. In reality, viscous terms (which are of order α^2 in the alpha disk) break the hydrostatic equilibrium and cause the equations of motion to form a system of nonlinear, coupled, second order partial differential equations which are rather challenging to solve (even numerically), but which bring the reward of a solution whose salient features cannot be described by height-integrated, i.e. ordinary, differential equations.

1.2. Equations of motion.

We use the generalized Navier Stokes equations, along with the equation of continuity, to describe the accretion flow and to represent viscous interactions:

$$\rho\frac{d\vec{V}}{dt} + \rho(\vec{V}\cdot\vec{\nabla})\vec{V} = -\vec{\nabla}P - \rho\vec{\nabla}\psi + \vec{\nabla}\cdot\sigma, \tag{1.3}$$

$$\frac{\partial\rho}{\partial t} + \vec{\nabla}\cdot(\rho\vec{V}) = 0, \tag{1.4}$$

where ρ is mass density, P is pressure, $\vec{V}$ is the velocity vector of a fluid element, and ψ is the gravitational potential. The rank two viscous stress tensor, σ, is assumed to have the following Cartesian components (Landau & Lifshitz 1959):

$$\sigma_{jk} = \eta\left[\frac{\partial V_j}{\partial x_k} + \frac{\partial V_k}{\partial x_j} - \frac{2}{3}\delta_{jk}\vec{\nabla}\cdot\vec{V}\right] + \xi\delta_{jk}\vec{\nabla}\cdot\vec{V}, \tag{1.5}$$

where ξ is bulk viscosity and $\eta = \nu\rho$ is the dynamic viscosity coefficient, both of which are functions of the coordinates.

With the assumptions described in § 1.1, the equations of motion in cylindrical coordinates become

$$v_r\frac{\partial v_r}{\partial r}+v_z\frac{\partial v_r}{\partial z}-\Omega^2 r=-\frac{\partial\psi}{\partial r}-\frac{1}{\rho}\frac{\partial P}{\partial r}+\frac{1}{\rho}F_r, \tag{1.6}$$

$$\rho\frac{v_r}{r^2}\frac{\partial}{\partial r}(r^2\Omega)+\rho v_z\frac{\partial\Omega}{\partial z}=\frac{1}{r^3}\frac{\partial}{\partial r}\left(\eta r^3\frac{\partial\Omega}{\partial r}\right)+\frac{\partial}{\partial z}\left(\eta\frac{\partial\Omega}{\partial z}\right), \tag{1.7}$$

$$v_r\frac{\partial v_z}{\partial r}+v_z\frac{\partial v_z}{\partial z}=-\frac{\partial\psi}{\partial z}-\frac{1}{\rho}\frac{\partial P}{\partial z}+\frac{1}{\rho}F_z, \tag{1.8}$$

$$\frac{1}{r}\frac{\partial}{\partial r}(r\rho v_r)+\frac{\partial}{\partial z}(\rho v_z)=0, \tag{1.9}$$

where $\psi(r,z)$ is the gravitational potential given by eq. (1.1). F_r and F_z are respectively the r and z components of the divergence of the viscous stress tensor, i.e. the viscous force, and are given by:

$$F_r=\frac{2}{r}\frac{\partial}{\partial r}\left(\eta r\frac{\partial v_r}{\partial r}\right)-\frac{2\eta v_r}{r^2}+\frac{\partial}{\partial z}\left[\eta\left(\frac{\partial v_r}{\partial z}+\frac{\partial v_z}{\partial r}\right)\right]+\frac{\partial}{\partial r}\left[\left(\xi-\frac{2}{3}\eta\right)\left(\vec{\nabla}\cdot\vec{V}\right)\right], \tag{1.10}$$

$$F_z=\frac{\partial}{\partial z}\left(2\eta\frac{\partial v_z}{\partial z}\right)+\frac{1}{r}\frac{\partial}{\partial r}\left[\eta r\left(\frac{\partial v_r}{\partial z}+\frac{\partial v_z}{\partial r}\right)\right]+\frac{\partial}{\partial z}\left[\left(\xi-\frac{2}{3}\eta\right)\left(\vec{\nabla}\cdot\vec{V}\right)\right]. \tag{1.11}$$

1.3. Constants of integration.

Vertical integration of eq. (1.9), with the assumption of a steady state, yields an expression of the conservation of mass flow through cylinders. Usually this is written as $\dot{M}=-2\pi r\Sigma\overline{v_r}$ where $\dot{M}$ is the constant mass accretion rate through any cylinder (and hence onto the star), Σ is the surface density in the disk, and $\overline{v_r}$ is an effective (i.e. density-weighted, height-averaged) radial velocity. However, since we are interested in the z dependence of the radial velocity, v_r, we choose to write this important equation as

$$\dot{M}=-2\pi r\int_{-\infty}^{+\infty}\rho v_r\,dz\;=\;\text{constant}, \tag{1.12}$$

where by convention $\dot{M} > 0$ for accretion, i.e. for $\overline{v_r} < 0$. The quantity $\dot{M}$ will serve as an integral of the motion for our accretion flow.

Another constant is obtained if, in the same spirit, we vertically integrate the angular momentum equation (1.7). If we first multiply both sides by r^3 and integrate over z from $-\infty$ to $+\infty$, we obtain:

$$\int_{-\infty}^{+\infty}(r\rho v_r)\frac{\partial(r^2\Omega)}{\partial r}dz - \int_{-\infty}^{+\infty} r^3\Omega\frac{\partial(\rho v_z)}{\partial z}dz = \frac{\partial}{\partial r}\left[r^3\int_{-\infty}^{+\infty}\eta\frac{\partial\Omega}{\partial r}dz\right] + r^3\eta\frac{\partial\Omega}{\partial z}\Bigg|_{-\infty}^{+\infty} \quad (1.13)$$

where in deriving the second term on the left hand side we have performed an integration by parts and set the boundary term to zero since $\rho \to 0$ as $z \to \pm\infty$.

Using the equation of continuity (1.9), we can transform the entire left-hand side into $(\partial/\partial r)\int_{-\infty}^{+\infty} r^3\rho v_r\Omega dz$. The last boundary term involving $\partial\Omega/\partial z$ also vanishes because $\eta = \nu\rho \to 0$ as $|z| \to \infty$ and, finally, integration over r gives

$$\dot{J}(r) - C = -2\pi r^3\int_{-\infty}^{+\infty}\eta\frac{\partial\Omega}{\partial r}dz, \quad (1.14)$$

where $-\dot{J}(r)$ is the advection rate of angular momentum through a cylinder of radius r, C is a constant of integration, and the right-hand side is the net torque exerted by viscous interactions on the same cylinder. Note that this equation is exact for any azimuthally symmetric, steady flow in which no mass is exchanged through the surface at infinity ($z = \pm\infty$), and in which no angular momentum is carried radially by radiation (Kluźniak 1987).

Since we consider only cases when the accretion rate is never zero, we can introduce another constant $j_+ = C/\dot{M}$. The torque vanishes when this new constant is equal to the height-averaged specific angular momentum $\bar{j}$ (weighted with radial momentum flux) or, correspondingly, when the height-averaged radial derivative of the angular momentum (weighted with dynamic viscosity) vanishes. That is, we can

rewrite eq. (1.14) as:

$$\dot{M}(\bar{j} - j_+) = -2\pi r^3 \left[\int_{-\infty}^{+\infty} \eta dz\right] \overline{\frac{d\Omega}{dr}}, \tag{1.15}$$

where $\dot{J}(r) = -2\pi r^3 \left(\int_{-\infty}^{+\infty} \rho v_r \Omega dz\right) = \dot{M}\bar{j}$, etc. If Ω is independent of z (i.e. constant on cylinders), the usual form of eq. (1.15) is recovered by removing the bars. Thus j_+ can be interpreted as the specific angular momentum at the zero-torque radius, r_m. For this reason, we now define a new effective radius, r_+, at which the Keplerian specific angular momentum is equal to j_+, i.e. $\sqrt{GM_* r_+} = j_+ = \Omega(r_m) r_m^2$. Note that in general the maximum value of Ω is not equal to the corresponding Keplerian value, $\Omega(r_m) \neq \Omega_k(r_m)$, and hence we do <u>not</u> expect r_+ to be the same as r_m.

1.4. The polytropic sound speed.

In the standard theory of thin accretion disks, the local sound speed becomes of prime importance when modeling subsonic accretion. A clear advantage of employing a barytropic equation of state is that it reduces the number of variables by one. A polytropic equation of state also greatly simplifies calculation of the local sound speed, i.e.

$$c_s^2 = \frac{dP}{d\rho} = \left(1 + \frac{1}{n}\right) \frac{P}{\rho}. \tag{1.16}$$

With the above relation we can rewrite the pressure gradients in eqs. (1.6) & (1.8) in terms of c_s, giving the following elegant expressions:

$$\frac{1}{\rho}\frac{\partial P}{\partial r} = n\frac{\partial c_s^2}{\partial r} \quad ; \quad \frac{1}{\rho}\frac{\partial P}{\partial z} = n\frac{\partial c_s^2}{\partial z}. \tag{1.17}$$

Now it is easy to show a basic result concerning a fluid in hydrostatic equilibrium in both the radial and vertical directions. Here eqs. (1.6) & (1.8), without the inertial

and viscous terms, reduce to a simple form involving only c_s, Ω, and ψ:

$$-\Omega^2 r = -\frac{\partial \psi}{\partial r} - n\frac{\partial c_s^2}{\partial r}, \tag{1.18}$$

$$0 = -\frac{\partial \psi}{\partial z} - n\frac{\partial c_s^2}{\partial z}. \tag{1.19}$$

Taking $\partial/\partial r$ of eq. (1.19) and $\partial/\partial z$ of eq. (1.18), we obtain the familiar result that $\partial\Omega/\partial z$=0, i.e. Ω is constant on cylinders for a polytrope in hydrostatic equilibrium (*cf.* Tassoul 1978). Since in eq. (1.7) the velocities are proportional to the viscosity, this already implies that in a barytropic disk of any thickness Ω is independent of z to leading order in a Taylor expansion in the (small) viscosity parameter (except, possibly, when the specific angular momentum is constant, $j \equiv r^2\Omega = \text{const.}$). We will perform a systematic expansion in a different small parameter, the dimensionless disk thickness, but for subsonic flow the same zeroth order result will be recovered.

1.5. Scaling the equations of motion.

At this point it is of paramount importance that we scale all relevant quantities by their corresponding characteristic values. This will make the equations dimensionless and allow us to weigh the relative significance of each term that appears. Following Regev (1983) we scale all velocities (v_z, v_r, and c_s) by the characteristic sound speed, $\tilde{c_s}$, all radial distances by some characteristic radius $\tilde{R}$ (e.g. R_*), and all vertical distances by $\tilde{H}$, the typical vertical scale height in the disk. We also represent Ω in units of $(GM_*/\tilde{R}^3)^{1/2} \equiv \Omega_{k*}$, the Keplerian angular velocity at the characteristic radius, and ρ in terms of a typical value $\tilde{\rho}$. Similarly, we scale the pressure by $\tilde{P} = \tilde{\rho}\,\tilde{c_s}^2$, the kinematic viscosity by $\tilde{\nu} = \tilde{c_s}\tilde{H}$, and the dynamic and bulk viscosity coefficient by $\tilde{\zeta} = \tilde{\eta} = \tilde{\nu}\,\tilde{\rho}$.

To apply a perturbative expansion technique to each equation we define an expansion parameter, ϵ. Since we are interested in geometrically thin disks we choose

$$\epsilon = \frac{\tilde{H}}{\tilde{R}} = \frac{\tilde{c_s}}{\Omega_{k*}\tilde{R}} \ll 1, \tag{1.20}$$

where we have used $\tilde{c_s} = \tilde{H}\Omega_{k*}$, in agreement with the standard result from thin disk theory that $H \sim c_s/\Omega_k$. In effect, ϵ is a parameter which measures the relative "thinness" of the disk.

Denoting the scaled forms of v_r and v_z by u and v respectively, we obtain the following set of non-dimensional equations:

$$\begin{aligned}\epsilon^2 u\frac{\partial u}{\partial r} + \epsilon v\frac{\partial u}{\partial z} - \Omega^2 r = &-\frac{1}{r^2}\left[1+\epsilon^2\left(\frac{z}{r}\right)^2\right]^{-3/2} - \epsilon^2\left(n\frac{\partial c_s^2}{\partial r}\right) - \epsilon^3\left(\frac{2\eta u}{\rho r^2}\right)\\ &+\frac{\epsilon^3}{\rho r}\frac{\partial}{\partial r}\left(2\eta r\frac{\partial u}{\partial r}\right) + \frac{\epsilon}{\rho}\frac{\partial}{\partial z}\left(\eta\frac{\partial u}{\partial z}\right) + \frac{\epsilon^2}{\rho}\frac{\partial}{\partial z}\left(\eta\frac{\partial v}{\partial r}\right)\\ &+\frac{\epsilon^3}{\rho}\frac{\partial}{\partial r}\left[\left(\xi-\frac{2}{3}\eta\right)\left(\frac{1}{r}\frac{\partial}{\partial r}(ru)\right)\right] + \frac{\epsilon^2}{\rho}\frac{\partial}{\partial r}\left[\left(\xi-\frac{2}{3}\eta\right)\frac{\partial v}{\partial z}\right],\end{aligned} \tag{1.21}$$

$$\epsilon\frac{\rho u}{r^2}\left[\frac{\partial}{\partial r}(r^2\Omega)\right] + \rho v\frac{\partial\Omega}{\partial z} = \epsilon^2\left[\frac{1}{r^3}\frac{\partial}{\partial r}\left(\eta r^3\frac{\partial\Omega}{\partial r}\right)\right] + \frac{\partial}{\partial z}\left(\eta\frac{\partial\Omega}{\partial z}\right), \tag{1.22}$$

$$\begin{aligned}\epsilon u\frac{\partial v}{\partial r} + v\frac{\partial v}{\partial z} = &-\frac{z}{r^3}\left[1+\epsilon^2\left(\frac{z}{r}\right)^2\right]^{-3/2} - n\frac{\partial c_s^2}{\partial z} + \frac{2}{\rho}\frac{\partial}{\partial z}\left(\eta\frac{\partial v}{\partial z}\right)\\ &+\frac{\epsilon^2}{\rho r}\frac{\partial}{\partial r}\left(\eta r\frac{\partial v}{\partial r}\right) + \frac{\epsilon}{\rho}\frac{\partial}{\partial z}\left[\left(\xi-\frac{2}{3}\eta\right)\left(\frac{1}{r}\frac{\partial}{\partial r}(ru)\right)\right]\\ &+\frac{1}{\rho}\frac{\partial}{\partial z}\left[\left(\xi-\frac{2}{3}\eta\right)\frac{\partial v}{\partial z}\right] + \frac{\epsilon}{\rho r}\frac{\partial}{\partial r}\left(\eta r\frac{\partial u}{\partial z}\right),\end{aligned} \tag{1.23}$$

$$\frac{\epsilon}{r}\frac{\partial}{\partial r}(r\rho u) + \frac{\partial}{\partial z}(\rho v) = 0, \tag{1.24}$$

where we have used eq. (1.17) in rewriting the pressure gradients. Here eqs. (1.21), (1.22), and (1.23) are the scaled radial, angular, and vertical momentum equations respectively and eq. (1.24) is the scaled form of the continuity equation. Armed with

the knowledge that $\epsilon \ll 1$ for a thin disk, we make eqs. (1.21)-(1.24) the foundation of our analysis and proceed to perturbatively expand all dynamical quantities in powers of ϵ. We will find $u \sim \epsilon$, $v \sim \epsilon^2$, i.e., $v_r = \mathcal{O}(\epsilon^2)v_\phi$ and $v_z = \mathcal{O}(\epsilon^3)v_\phi$; therefore the divergence terms $\nabla \cdot \vec{V}$ in eq. (1.5) contribute at order not lower than ϵ^3 to eqs. (1.6) and (1.8)—this formally justifies their frequent neglect.

2. Solution for the vertical structure by perturbative expansion in ϵ.

2.1. Power series in $\epsilon = \tilde{H}/\tilde{R}$.

We expand all variables in powers of ϵ and will evaluate eqs. (1.21)-(1.24) at various orders. We let

$$(\Omega/\Omega_{k*}) = \Omega_0 + \epsilon\Omega_1 + \epsilon^2\Omega_2 + ..., \tag{2.25}$$

$$u = (v_r/\tilde{c_s}) = u_0 + \epsilon u_1 + \epsilon^2 u_2 + ..., \tag{2.26}$$

$$v = (v_z/\tilde{c_s}) = v_0 + \epsilon v_1 + \epsilon^2 v_2 + ..., \tag{2.27}$$

as well as $(c_s/\tilde{c_s}) = c_{s0} + \epsilon c_{s1} + \epsilon^2 c_{s2} + ...$, and $(\rho/\tilde{\rho}) = \rho_0 + \epsilon\rho_1 + \epsilon^2\rho_2 + ...$, with the assumption that the dimensionless vertical scale height of the disk, $h(r) = H(r)/\tilde{H}$, is of order unity, $h \sim \mathcal{O}(1)$. All other variables like P, η, ν, & $\dot{M}$ can be expressed in terms of these six fundamental quantities[2]. Our objective then is to calculate, order by order in ϵ, the functional dependence of Ω, u, v, c_s, ρ, and h on the coordinates r and z alone.

[2]In reality only five of these are independent for a polytrope since eq. (1.16) gives c_s in terms of ρ (or vice-versa).

Assumption ii) of § 1.1, regarding reflection symmetry about the ($z = 0$) midplane, implies that physical quantities such as Ω, ρ, P, η, u, and c_s are even functions of z, while v is odd under reflections through the equatorial plane. When we expand an even/odd function (e.g. Ω) in powers of $\epsilon \ll 1$, we require each term in the expansion (e.g. Ω_i; $i = 0, 1, 2,...$) to be independently even/odd.

2.2. Viscosity-independent zeroth order results for the vertical structure.

Examination of eq. (1.21) at zeroth order immediately gives

$$\Omega_0 = r^{-3/2}, \tag{2.28}$$

i.e. Ω_0 is equal to the Keplerian value at the midplane, $\Omega_k \equiv v_{\phi k}/r \equiv \sqrt{GM_*/r^3}$ in conventional units. Though eq. (2.28) is consistent with the assumption of a rotationally supported disk, it cannot satisfy the inner boundary condition of $\Omega(r_*) = \Omega_*$ whenever the star rotates below its Keplerian value at the stellar radius, nor the more general zero-torque boundary condition. Clearly, our perturbative solution will be invalid in the limit $r \to r_+$. This is because implicit in the scaling of § 1.5 has been the assumption that $\partial/\partial r \sim \epsilon(\partial/\partial z)$. This approximation, however, is known to be patently false in the inner transition region between the central star and the Keplerian portion of the disk.

Eq. (1.24), the equation of continuity, fixes v at zeroth order to be zero everywhere, $v_0 = 0$. To see this more clearly, observe that $\partial(\rho_0 v_0)/\partial z = 0$ and so $\rho_0 v_0$, the lowest order vertical component of the mass flow, is a function of r only. However, since v is odd with respect to the z coordinate, we know $\rho_0 v_0 = 0$ for all points on the midplane ($z = 0$) and, not being a function of z, this product must then vanish everywhere. Clearly $\rho_0 \neq 0$ and thus $v_0 = 0$ at all points in the rotationally supported disk.

Moving on to first order in ϵ for the angular velocity, we see that because Ω is even with respect to reflections through the midplane, the first order correction to the angular velocity vanishes, $\Omega_1 = 0$. This result for Ω_1 also has direct impact on the fluid velocities, since eqs. (1.22) & (1.24) at order ϵ now give $u_0 = v_1 = 0$. Using this result for u and v, we then find that the only surviving term of order ϵ in eq. (1.23) involves the first order correction to the square of the sound speed, and thus $c_{s1}^2 = 0$, and hence $\rho_1 = P_1 = 0$, which is consistent with symmetry arguments for these three quantities. With this information, eq. (1.23) simply becomes the standard equation of vertical hydrostatic equilibrium:

$$\frac{1}{\rho_0}\frac{\partial P_0}{\partial z} = n\frac{\partial (c_{s0}^2)}{\partial z} = -\frac{z}{r^3}. \tag{2.29}$$

We can solve eq. (2.29), i.e. the vertical momentum equation up to corrections of order ϵ^2, and hence find c_{s0}, ρ_0, and P_0. In the case of polytropic index $n = 3/2$ we obtain the following relations (Hōshi, 1977):

$$c_{s0}(r,z) = \sqrt{\frac{h^2 - z^2}{3r^3}}, \tag{2.30}$$

$$\rho_0(r,z) = \left(\frac{h^2 - z^2}{5r^3}\right)^{3/2}, \tag{2.31}$$

$$P_0(r,z) = \rho_0^{5/3} = \left(\frac{h^2 - z^2}{5r^3}\right)^{5/2}. \tag{2.32}$$

Eqs. (2.31)-(2.32) show that $h(r)$ is now the height at which $\rho = 0$ (and hence $P = 0$), implying that h is the true semi-thickness of the disk, though its functional dependence on r is still undetermined. The surface density, $\Sigma(r)$, can also be derived in terms of h to lowest order in ϵ:

$$\Sigma_0(r) = \int_{-h}^{+h} \rho_0 \, dz = \frac{3\pi}{40\sqrt{5}}\left(\frac{h^4}{r^{9/2}}\right), \tag{2.33}$$

where we have replaced the integration limits of $\pm\infty$ by $\pm h$, since by eq. (2.31) the polytropic disk terminates at $z = \pm h(r)$.

It is now possible to put the integrated mass continuity equation (1.12) into dimensionless form. Scaling as before and using the fact that to lowest non-vanishing order in ϵ, $u = \epsilon u_1 + ...$ and $\rho = \rho_0 + ...$, we can write eq. (1.12) to lowest order in ϵ:

$$\epsilon \dot{m} = -r \int_{-h}^{+h} \rho u \, dz \sim -\epsilon \, r \int_{-h}^{+h} \rho_0 u_1 \, dz, \tag{2.34}$$

where $\dot{m} = \dot{M}/(2\pi\tilde{\rho}\tilde{c_s}\tilde{H}^2) \sim \mathcal{O}(1)$, is a dimensionless constant. For an adiabatic index of $n = 3/2$, eq. (1.2) gives $\tilde{\rho} \sim K^{-3/2}\tilde{c_s}^3$ and, since $\tilde{H} \sim \tilde{c_s}/\Omega_{k*}$, we find $\dot{m} \sim \dot{M}/\tilde{c_s}^6$. Because $\dot{m}$ is independent of ϵ for $u_1 \neq 0$, this implies that the unscaled mass accretion rate must scale as $\dot{M} \sim \mathcal{O}(\epsilon^6)$, and hence $\dot{M}$ depends sensitively on the relative "thinness" of the disk. As we shall soon see, the scaled eq. (2.34) is of prime importance in determining the vertical structure and must therefore be included with eqs. (1.21)-(1.24).

Up to this point, all the results obtained in this section, including eqs. (2.28) and (2.30)-(2.33), are common to the outer regions ($r >> r_+$) of any standard thin disk with polytropic equation of state, for any viscosity prescription. However, all of these expressions depend intrinsically on the vertical scale height, $h(r)$, which cannot be determined as an explicit function of r without a form for $\eta(r, z)$ being first specified. We cannot obtain solutions for the lowest non-vanishing orders in ϵ of v_r and v_z, nor can we evaluate the first nonzero correction to Ω without specifying the viscosity prescription.

2.3. Lowest-order results using the standard α-disk prescription.

Let us continue all calculations under the assumption that the viscosity is given by the α-disk formulation. In view of the large uncertainty in modeling the kinematic viscosity, authors in the past have generally neglected any z dependence for ν.

Laboratory studies of turbulent jets undergoing free expansion lend some support to this hypothesis (*cf.* Urpin 1984a, Monin & Yaglom 1965). However, we find this to be unacceptable when solving for $v_r(r,z)$ and $v_z(r,z)$ in a polytropic disk as it leads to divergent expressions at the surface of the disk, $v(r,\pm h) \to \infty$ (Kita 1995). We choose then to modify the alpha prescription by directly incorporating a form of z dependence into the kinematic viscosity. But first, to better demonstrate that the zeroth order results are hardly affected by the choice of the z dependence in the kinematic viscosity, let us write down the result for the height of the (polytropic) standard alpha disk, where $\partial\nu/\partial z = 0$ and

$$\nu = \alpha c_s H. \tag{2.35}$$

If c_s taken to be the zeroth order equatorial sound speed, $\bar{c}_{s0}(r) \equiv c_{s0}(r,0)$, one obtains the following zeroth order expressions for the kinematic and dynamic viscosity coefficients:

$$\bar{\nu}_0(r) = \frac{\alpha}{\sqrt{3}}\left(\frac{h^2}{r^{3/2}}\right), \tag{2.36}$$

$$\bar{\eta}_0(r,z) = \bar{\nu}_0\rho_0 = \frac{\alpha}{5\sqrt{15}}\left[\frac{h^2\left(h^2-z^2\right)^{3/2}}{r^6}\right]. \tag{2.37}$$

Notice that with this standard α-disk viscosity law, ν_0 depends solely on r and, therefore, η_0 inherits its z dependence entirely from the density, $\rho_0(r,z)$, as given by eq. (2.31).

Now the disk semi-thickness, $h(r)$, can be determined as a function of radius. To do this we observe that through lowest order in ϵ, eq. (1.15) reads:

$$\dot{m}(j_0 - j_+) = -r^3\left[\int_{-h}^{+h}\eta_0 dz\right]\frac{d\Omega_0}{dr}, \tag{2.38}$$

where $\dot{m}$ is the scaled constant from eq. (2.34), $j_0 = r^{1/2}$ is the (zeroth order) Keplerian specific angular momentum, and $j_+ = r_+^{1/2}$ is the integration constant that arises from

the no-torque boundary condition[3] that accompanies eq. (1.15). Using eq. (2.37) for η_0 and integrating over z, we are left with the following simple algebraic equation for the dimensionless disk height, $h(r)$:

$$\frac{h(r)}{r} = \bar{\lambda}_0 \left(1 - \sqrt{\frac{r_+}{r}}\right)^{1/6} \qquad \text{with} \qquad \bar{\lambda}_0 = \left[\frac{\dot{m}}{\alpha}\left(\frac{80}{3\pi}\sqrt{\frac{5}{3}}\right)\right]^{1/6}. \tag{2.39}$$

This result implies that $h(r)/r \to \bar{\lambda}_0$ =constant as $r \to \infty$, and that the disk remains thin (i.e. $H(r)/r \sim \epsilon$) for all radii, provided, of course, that α is not too small. In addition, we see that as $r \to r_+$, $h \to 0$. This is a consequence of our using j_0 and $d\Omega_0/dr$ in eq. (2.38), despite the requirement that $d\Omega/dr \to 0$ as j (not j_0) $\to j_+$. As we will see in Section 4, this is in fact a signal that our use of eq. (2.38) to determine h is not appropriate in the neighborhood of r_+.

It should be pointed out that the results we have so far obtained in this and the previous subsection are well known (*cf.* Shakura & Sunyaev 1973, Hōshi 1977, Paczyński 1991). Novel developments only become apparent when eqs. (1.21)-(1.24) are solved to higher order. But, as already remarked, eqs. (2.36) and (2.37) cannot be used to consistently extend the results obtained so far to higher order, it is first necessary to slightly modify the viscosity prescription.

2.4. Lowest order results with height-dependent kinematic viscosity.

In the original paper by Shakura & Sunyaev (1973) the dominant component of the viscous stress tensor is presumed to have the following form:

$$\sigma_{r\phi} \sim \eta r(\partial\Omega/\partial r) \sim -\alpha P. \tag{2.40}$$

[3]If for some reason Ω_0 was a function of both r and z we would need to use eq. (1.14).

Since we know that in the outer disk $r(\partial\Omega/\partial r) \sim -\Omega_k$, we use eq. (2.40) as a guide to make the following assumption regarding the z dependence of the viscosity:

$$\nu(r,z) = \frac{\alpha}{\Omega_k}\left[\frac{c_s^2(r,z)}{(1+1/n)}\right], \tag{2.41}$$

consistent with $\eta(r,z) \sim \alpha P(r,z)/\Omega_k$ where $P \sim \rho c_s^2$ for a polytrope. Our new expression for $\nu(r,z)$ reduces to the original formulation of eq. (2.35) in the midplane of the disk ($z = 0$). We justify our choice of ν by noting that if the turbulent speed, v_{turb}, is bounded from above by the local sound speed, we must expect v_{turb} to vary considerably with height, since for a polytrope $c_s \to 0$ as $z \to \pm h$.

By using eqs. (2.30)-(2.32) & (2.41), we derive new forms for the zeroth order kinematic and dynamic viscosity coefficients:

$$\nu_0(r,z) = \frac{2\alpha}{15}\left[\frac{h^2 - z^2}{r^{3/2}}\right], \tag{2.42}$$

$$\eta_0(r,z) = \nu_0(r,z)\rho_0(r,z) = \frac{2\alpha}{75\sqrt{5}}\left[\frac{(h^2 - z^2)^{5/2}}{r^6}\right]. \tag{2.43}$$

Comparison of eq. (2.43) with eq. (2.37) shows that η_0 is now one power higher in $(h^2 - z^2)$ and, as shown by Kita 1995, it is this difference that is the key to suppressing the divergence of v_r and v_z at the disk surface.

We must first examine the impact that eqs. (2.42)-(2.43) may have on all other previously derived quantities. Since none of the results in § 2.2 depend in any way on ν or η, we know they are unaffected. The only change is in the value of the height of the disk (but not its functional form), which is increased by a factor $3^{1/4}$:

$$\frac{h(r)}{r} = \lambda\left(1 - \sqrt{\frac{r_+}{r}}\right)^{1/6} \quad \text{with} \quad \lambda = \left[\frac{\dot{m}}{\alpha}\left(\frac{16(5)^{3/2}}{\pi}\right)\right]^{1/6} \approx 1.96\left(\frac{\dot{m}}{\alpha}\right)^{1/6}. \tag{2.44}$$

2.5. Second order disk equations.

To explore the differential rotation with respect to z and the nature of the velocity vector field in the accretion disk, we now consider only terms of $\mathcal{O}(\epsilon^2)$ in eqs. (1.21)-(1.22). Bearing in mind that $\Omega_0 = r^{-3/2}$, $\Omega_1 = 0$, and $u_0 = v_0 = v_1 = 0$, we discover the following equations for Ω_2, u_1, and v_2:

$$-2\Omega_0\Omega_2 r = \frac{3}{2}\frac{z^2}{r^4} - \frac{3}{2}\frac{\partial c_{s0}^2}{\partial r} + \frac{1}{\rho_0}\frac{\partial}{\partial z}\left(\eta_0\frac{\partial u_1}{\partial z}\right), \tag{2.45}$$

$$r\rho_0 u_1 \frac{d\left(r^2\Omega_0\right)}{dr} = \frac{\partial}{\partial r}\left(\eta_0 r^3\frac{d\Omega_0}{dr}\right) + r^3\frac{\partial}{\partial z}\left(\eta_0\frac{\partial\Omega_2}{\partial z}\right), \tag{2.46}$$

$$\frac{1}{r}\frac{\partial}{\partial r}(r\rho_0 u_1) + \frac{\partial}{\partial z}(\rho_0 v_2) = 0. \tag{2.47}$$

Here, c_{s0}, ρ_0 and η_0 are given by eqs. (2.30), (2.42) and (2.43), and h is known up to the integration constant r_+. Unfortunately, the two viscous terms at the end of eqs. (2.45) & (2.46) complicate things by coupling the two equations together. To simplify the equations, most authors assume *a priori* that Ω and v_r in the outer disk are both functions of only r. As we will show, this is justified only in the limit $\alpha << \epsilon$. We prefer to keep all terms so that we can obtain a solution valid through order ϵ^3 which is consistent for all values of α.

2.6. Complete analytical solution for Ω_2, u_1, and v_2.

To solve for Ω_2 and u_1, we will make the ansatz that $u_1(r,z) = f_1(r)(h^2 - z^2) + f_2(r)$, where $f_1(r)$ and $f_2(r)$ are as yet undetermined functions of r. A heuristic justification for this choice is that if the equations are decoupled by neglecting the z derivatives, as in the olden approach common in the

literature, the solution for the lowest order corrections to Keplerian motion are

$$\frac{\Omega_2|^{old}(r)}{\Omega_0} = -\frac{3}{4}\left(\frac{h}{r}\right)^2\left[1-\frac{2}{3}\left(\frac{d\ln h}{d\ln r}\right)\right], \tag{2.48}$$

and $u_1|^{old}(r,z) = g_1(r)(h^2-z^2)+g_2(r)$, where

$$g_1(r) = \left(\frac{11}{5}\right)\frac{\alpha}{r^{5/2}} \qquad \text{and} \qquad g_2(r) = -2\alpha\left(\frac{h^2}{r^{5/2}}\right)\left(\frac{d\ln h}{d\ln r}\right). \tag{2.49}$$

Given the nature of the coupling term, $\eta_0(\partial u_1/\partial z)$, in eq. (2.45), it is now possible to formulate Ω_2 in terms of $f_1(r)$ and $f_2(r)$, i.e.

$$\Omega_2(r,z) = \Omega_2|^{old}(r) + \frac{2}{15}\alpha\left(\frac{f_1(r)}{r}\right)(h^2-6z^2). \tag{2.50}$$

We then solve for $f_1(r)$ and $f_2(r)$ by substituting eq. (2.50) directly into the term involving $\eta_0(\partial\Omega_2/\partial z)$ that appears in eq. (2.46). This results in the following forms for the radial functions:

$$f_1(r) = \frac{g_1(r)}{\left(1+\frac{64}{25}\alpha^2\right)} \qquad \text{and} \qquad f_2(r) = \left(\frac{32}{15}\alpha^2\right)\left(\frac{g_1(r)h^2}{1+\frac{64}{25}\alpha^2}\right)+g_2(r), \tag{2.51}$$

where the functions $g_1(r)$ and $g_2(r)$ are defined by eq. (2.49). In this way we finally obtain complete solutions for Ω_2 and u_1 in closed analytical form:

$$\frac{\Omega_2(r,z)}{\Omega_0} = \left(\frac{h}{r}\right)^2\left[-\frac{3}{4}+\frac{1}{2}\left(\frac{d\ln h}{d\ln r}\right)+\frac{2}{15}\alpha^2\Lambda\left(1-6\frac{z^2}{h^2}\right)\right], \tag{2.52}$$

$$u_1(r,z) = -\alpha\left(\frac{h^2}{r^{5/2}}\right)\left[-\Lambda\left(1-\frac{z^2}{h^2}\right)-\Lambda\left(\frac{32\alpha^2}{15}\right)+2\left(\frac{d\ln h}{d\ln r}\right)\right], \tag{2.53}$$

where Λ is a constant that depends on the parameter α and is given by

$$\Lambda = \frac{11}{5}\Big/\left(1+\frac{64}{25}\alpha^2\right). \tag{2.54}$$

Note that $\Omega_2(r,z)$ exhibits differential rotation with respect to the vertical coordinate; a feature which was also observed in the numerical solution by Kley &

Lin (1992).This is because by including the viscous term of $\eta_0(\partial u_1/\partial z)$ in the radial momentum equation we are no longer solving for Ω under an assumption of strict radial hydrostatic equilibrium.

We also observe that in the limit of $\alpha \ll 1$, so that α^2 is a vanishingly small quantity, eqs. (2.52)-(2.53) reduce identically to the solutions for Ω_2 and u_1 of the equations of motion without the coupling terms. This suggests that neglecting the viscous coupling terms is justified, so long as α is not too large, i.e. $\alpha \leq \epsilon$. However, when $\alpha \sim 10^{-1}$ to 1, the effects of including the $\mathcal{O}(\epsilon^2)$ viscous terms becomes readily apparent.

Note that $u_1(r,z)$, being quadratic in z, is an even function with respect to reflections through the midplane ($z = 0$). It is also clear, upon reinstating the appropriate scale factors, that $v_r/v_{\phi k} \sim H^2/r^2 \sim \epsilon^2$ in the outer disk, where our use of eq. (2.44) for the disk surface is known to be valid. Since $(d\ln h/d\ln r)$ diverges at r_+, we observe that $\lim_{r\to r_+} u_1(r,z) \to -\infty$, i.e. we have not cured the well known divergence of the Shakura–Sunyaev disk at the zero torque radius: as $r \to r_+$, $h \to 0$, $\rho \to 0$ and, to preserve $\dot{M}$ =const, $v_r \to \infty$. However, for all radii $r > r_+$, u is finite everywhere and on the surface of the disk has the finite nonzero value given by

$$u_1(r,\pm h) = -\alpha\left(\frac{h^2}{r^{5/2}}\right)\left[2\left(\frac{d\ln h}{d\ln r}\right) - \frac{352\alpha^2}{3(25+64\alpha^2)}\right] < 0. \qquad (2.55)$$

With the knowledge that u_1 remains finite at the surface of the disk, we can now pursue, with confidence, a solution for the lowest non-vanishing order of v_z, i.e. v_2, by means of eq. (2.47), the equation of continuity up through second order in ϵ. If we use eq. (2.31) for ρ_0 and eq. (2.53) for u_1, then after the requisite differentiation (with respect to r) and integration (with respect to z), we can determine $v_2(r,z)$ up to an unknown function of the disk radius. Yet since v_z is an odd function of z and therefore $v_2 = 0$ in the equatorial plane for all r, this implies that the unknown function of r

must be zero everywhere in the disk. In this manner, we find the following unique solution for v_2:

$$v_2(r,z) = -\alpha\left(\frac{z}{r}\right)\left(\frac{h^2}{r^{5/2}}\right)\left[-\Lambda\left(1-\frac{z^2}{h^2}\right) - \frac{32\alpha^2\Lambda}{15}\left(\frac{d\ln h}{d\ln r}\right) + 2\left(\frac{d\ln h}{d\ln r}\right)^2\right] \quad (2.56)$$

where Λ is the same constant that appears in eq. (2.54).

We immediately notice several important features of the solution. First, as with $\Omega_2(r)$ and $u_1(r,z)$, $\lim_{r\to r_+} v_2(r,z) \to -\infty$ because of its dependence on $(d\ln h/d\ln r)^2$. Secondly, we see that $|v_z/v_r| \sim H/r \sim \epsilon$, as was expected for a standard thin disk in vertical hydrostatic equilibrium. Finally, v_2, like u_1, is finite along the surface of the disk for all r, i.e.

$$v_2(r,\pm h) = \mp\alpha\left(\frac{h^3}{r^{7/2}}\right)\frac{d\ln h}{d\ln r}\left[2\left(\frac{d\ln h}{d\ln r}\right) - \frac{352\alpha^2}{3(25+64\alpha^2)}\right]. \quad (2.57)$$

We now check our solutions to see if they concur with what we expect for a standard thin disk. First, it is possible to show that eq. (2.53) satisfies eq. (2.34) for the vertically-integrated mass flux, $\dot{m}$, even with the unexpected dependence on α^2. Second, a quick glance reveals that our new solutions for Ω_2, u_1, and v_2 have the necessary parities with respect to reflection through the $(z=0)$ midplane, i.e. even, even, and odd, respectively. Third, if we replace the appropriate dimensional units for each quantity, we see that $(v_\phi - v_{\phi k})/v_{\phi k}$ and $v_r/v_{\phi k}$ are both of $\mathcal{O}(\epsilon^2)$, while $v_z/v_{\phi k}$ is $\mathcal{O}(\epsilon^3)$; all of which is entirely in complete agreement with our assumption that the flow in the outer portions of the disk is predominantly Keplerian.

Finally, since $h(r)$ is the semi-thickness of the disk, we must have $v_z/v_r = \pm(dh/dr)$ for all points $(r,\pm h)$ on the surface of the disk, as otherwise the geometrical disk surface cannot be in a steady-state. Comparison of eqs. (2.55) & (2.57) shows that this constraint is indeed satisfied for the lowest non-vanishing orders of v_r and v_z:

$$\pm\frac{v_2(r,\pm h)}{u_1(r,\pm h)} = \left(\frac{h}{r}\right)\left(\frac{d\ln h}{d\ln r}\right) = \frac{dh}{dr}. \quad (2.58)$$

We stress that the new solutions for Ω_2, u_1, and v_2 fully comply with the above list of conditions for all possible values of α, provided that the disk remains geometrically thin. The remaining properties of eqs. (2.52)-(2.57) for Ω_2, u_1, and v_2 will be discussed in detail in the following section.

3. Detailed discussion of analytical results.

In this section we examine the detailed properties of Ω_2 (eq. [2.52]), and in §4 those of the remaining components of the vector field, u_1, and v_2, eqs. (2.53)-(2.57). Since by assumption ii) (§§1.1, 2.1) the next order corrections vanish everywhere in the disk, $\Omega_3 = u_2 = v_3 = 0$, our equations are valid up to corrections of $\mathcal{O}(z^4/r^4)$ for Ω and v_r, and $\mathcal{O}(z^5/r^5)$ for v_z. In other words, the results we describe are valid in the outer disk ($r > 1.4r_+$) up to relative corrections of ϵ^2, e.g. for $H/R \approx 0.1$ the expressions are valid to 1%.

In § 3.1, we study the nature of the z dependence of $\Omega_2(r, z)$. In § 3.3 we also discuss the interpretation of the apparent singularity in Ω_2 at $r = r_+$. In § 4, we look at the velocity vector field in the outer disk, paying special attention to the sign of v_r and v_z. We find that beyond a certain radius there is significant mass outflow near the equatorial plane for a wide range of α's. We carefully analyze all of its important characteristics, including, in § 4.3, the fraction of the total mass flow carried out to infinity by this phenomenon.

3.1. Analysis of the lowest-order correction to Ω.

We found that the angular velocity of material in the disk, up to and including terms of $\mathcal{O}(\epsilon^2)$ is given by

$$\Omega = \Omega_0 \left\{ 1 + \epsilon^2 \left(\frac{h}{r} \right)^2 \left[-\frac{3}{4} + \frac{1}{2} \left(\frac{d \ln h}{d \ln r} \right) + \frac{2}{15} \alpha^2 \Lambda \left(1 - 6 \frac{z^2}{h^2} \right) \right] \right\}. \tag{3.59}$$

Eq. (3.59) for Ω is valid up to corrections of $\mathcal{O}(z^4/r^4)$ for a geometrically thin disk.

As pointed out in Ch. 2 Ω is clearly an even function of z and is Keplerian up through first order in ϵ. In addition, since $\lim_{r\to\infty}(d \ln h/d \ln r) = 1$ and $\lim_{r\to\infty}(h/r) = \lambda$ from eq. (2.44), we find that

$$\lim_{r\to\infty} \left(\frac{\Omega}{\Omega_0} - 1 \right) = \epsilon^2 \lambda^2 \left[-\frac{1}{4} + \frac{2}{15} \alpha^2 \Lambda \left(1 - 6 \frac{z^2}{h^2} \right) \right]. \tag{3.60}$$

Note that this limit is negative for all z because $0 \leq 2\alpha^2\Lambda/15 \leq 0.082$ over the range $0 \leq \alpha \leq 1$. Also observe that in the case of $\alpha \ll 1$, eq. (3.60) reduces to a negative constant $-\epsilon^2\lambda^2/4$. Thus, in the limit of inviscid flow ($\alpha \to 0$), Ω is constant on cylinders (but subkeplerian for $r >> r_+$). Finally, because $h^2(d \ln h/d \ln r) \to \infty$ as $r \to r_+$, we know that Ω, as given by eq. (3.59), diverges at $r = r_+$. It is on these last two properties that we now focus our attention.

3.2. Differential rotation of the angular velocity with respect to z.

In this subsection, we discuss the z dependence of Ω. We define the quantity $\Delta\Omega = [\Omega(r, \pm H) - \Omega(r, 0)]$ to be the difference between the angular velocity at the surface of the disk and the angular velocity in the equatorial plane. From eq. (3.59), we derive the following expression for the fractional difference:

$$(\Delta\Omega/\Omega_0) = -\frac{\epsilon^2}{\Omega_0} \left[\Omega_2(r, \pm h) - \Omega_2(r, 0) \right] = -\epsilon^2 \left(\frac{h}{r} \right)^2 \left(\frac{4}{5} \alpha^2 \Lambda \right). \tag{3.61}$$

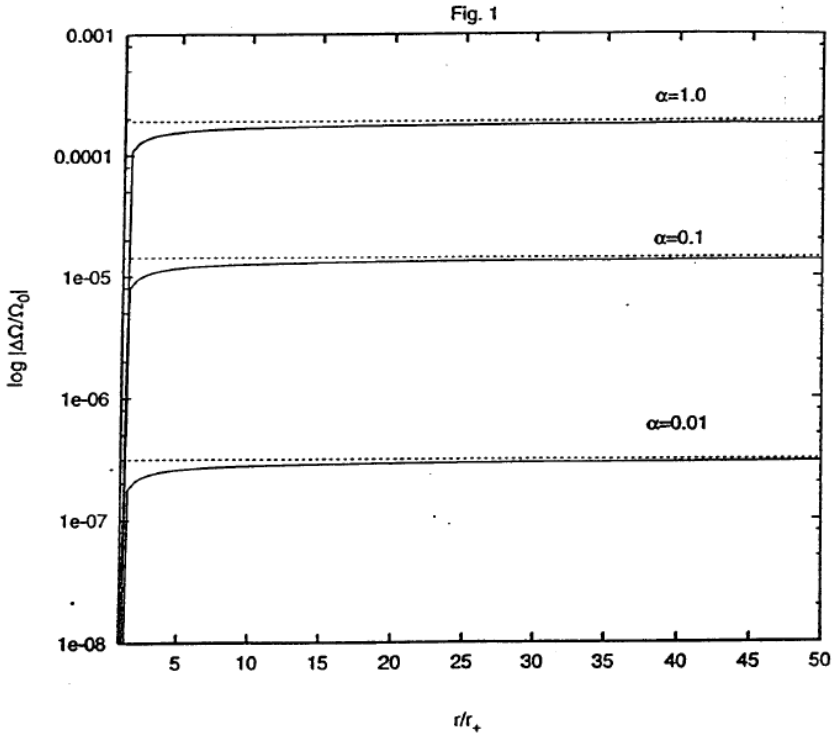

Fig. 1.— The fractional difference between the angular velocity at the disk surface and the angular velocity in the equatorial plane relative to Keplerian as a function of the radius, for $\epsilon = 0.01$ and α =0.01, 0.1, 1.0. The dashed lines correspond to $\lim_{r\to\infty} \log|\Delta\Omega/\Omega_0|$. Note that in all the figures we arbitrarily choose $\dot{m} = 1$.

Clearly, this fraction is negative for all radii. In Fig. 1, we plot $\log|\Delta\Omega/\Omega_0|$ in the disk with $\epsilon = 0.01$ and $\dot{m} = 1$, for several values of the viscosity parameter: $\alpha = 0.01$, 0.1, and 1.0. We observe that in the limit of $r \gg r_+$, since $\lim_{r\to\infty}(h/r) = \lambda$ (see eq. (2.39)), the fractional difference in Ω tends to a negative constant given by $\lim_{r\to\infty}(\Delta\Omega/\Omega_0) \to -\epsilon^2(4/5)\alpha^2\Lambda\lambda^2$ (dashed lines).

The amount by which the surfaces of constant Ω deviate from upright cylinders is proportional to ϵ^2 and therefore very small for a thin disk. The nearly constant behavior for $(\Delta\Omega/\Omega_0)$ for $r \gg r_+$ is also interesting in its own right since it implies that the total departure of the surfaces of constant Ω from the vertical does not significantly decrease (or increase) as one goes further out in the disk. Examination of eq. (3.61), also shows us that formally differential rotation vanishes as $r \to r_+$, since $h \to 0$ at $r = r_+$; however, as $\Omega = \Omega_0 + \epsilon^2\Omega_2$ diverges to $+\infty$ at $r = r_+$, this result of $\Delta\Omega \to 0$ really has no physical meaning.

3.3. The singularity in $\Omega(r, z)$ in the inner disk.

In Fig. 2(a), we plot the second order correction to Ω (i.e. $\epsilon^2\Omega_2$) as a function of r in the ($z = 0$) midplane for three different values of α. In Fig. 2(b), we plot $H = \epsilon h(r)$ for the same values α used in Fig. 2(a). For each choice of α, observe the singularity in Ω_2 at r_+. Clearly, as the presumed $\mathcal{O}(\epsilon^2)$ correction provided by Ω_2 grows without bound near $r = r_+$, the assumptions underlying our perturbative expansion are invalid there.

The reason for the divergence, at $r = r_+$, of Ω_2 , v_r and v_z can be traced back directly to the lowest order form of the vertically-integrated angular momentum

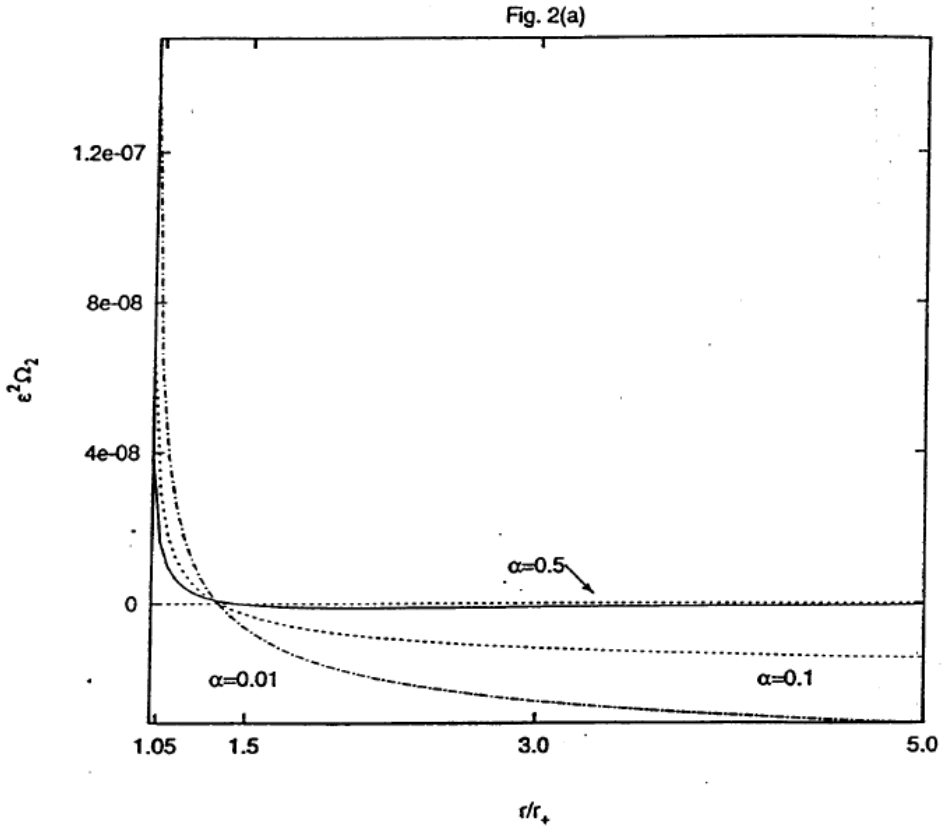

Fig. 2(a).— Plot of the second order correction to Ω vs. radius for $\epsilon = 0.01$ and $\alpha = 0.01, 0.1, 0.5$. Note the change in sign for $r \approx 1.4r_+$ for all three values of α.

equation (2.38):

$$\dot{m}(j_0 - j_+) = -r^3 \left[\int_{-h}^{+h} \eta_0 dz\right] \frac{d\Omega_0}{dr}. \tag{3.62}$$

The left side of eq. (3.62) is proportional to $(j_0 - j_+) = j_0 \left(1 - \sqrt{r_+/r}\right)$ and as such must vanish at $r = r_+$. Since we are still assuming that $\Omega \approx \Omega_0$ in the neighborhood of r_+, if the right side is to also vanish there, then it is necessary for the height-integrated viscosity, $\int_{-h}^{+h} \eta_0 dz$, to go to zero at $r = r_+$. However, in the α-disk prescription $\int_{-h}^{+h} \eta_0 dz$ is proportional to $(h/r)^6$, so this leads to the conclusion that $h \to 0$ as $r \to r_+$ (Shakura & Sunyaev 1973). This functional form of $h(r)$ causes a singularity in its derivative at r_+, i.e. $\lim_{r \to r_+}(dh/dr) \to +\infty$, and hence to a "cusp"

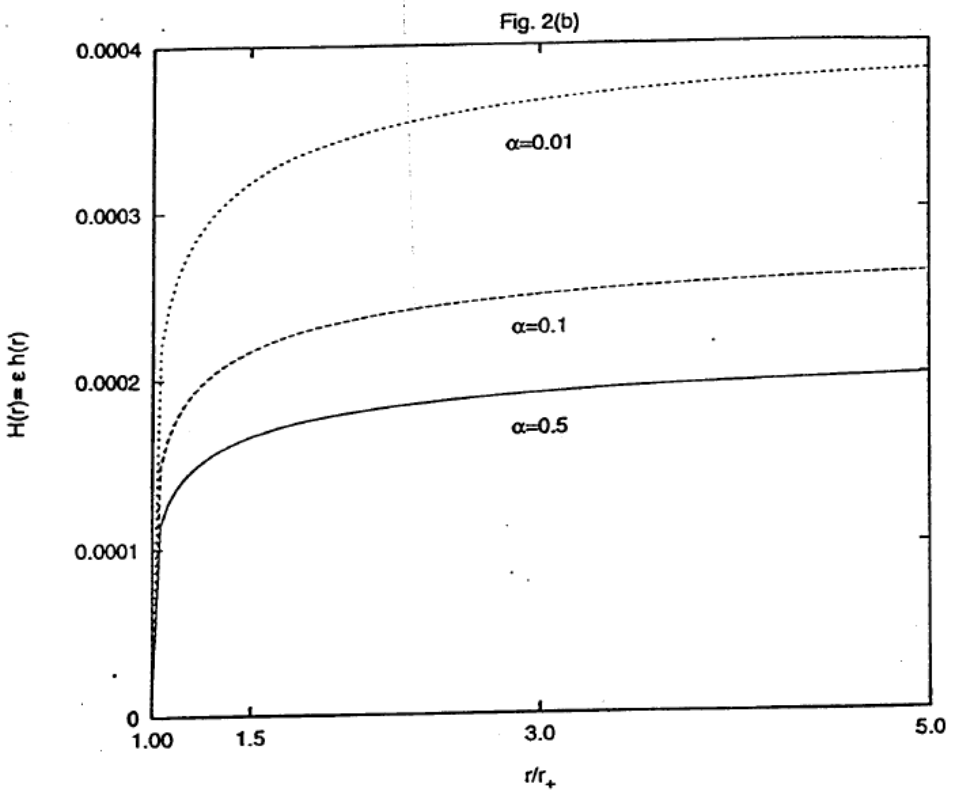

Fig. 2(b).— The surface of the disk, $H = \epsilon h(r)$, for the identical set of parameters used in Fig. 2(a). Observe that for all three values of α, the singularity in Ω in Fig. 2(a) at $r = r_+$ corresponds to $H \to 0$.

in the disk surface.

The fault for all of this lies in the assumption that one can continue the perturbative expansion into the transition region, near the zero-torque point, r_{max}, where Ω reaches a maximum. While it is true that eq. (1.15) holds for all radii, including $r = r_+$, the same cannot be said for its lowest order expansion in ϵ, eq. (3.62), which was used in the derivation of $h(r)$ and hence all other physical quantities. Since Ω is maximal at $r = r_{max}$, $\partial\Omega/\partial r \to 0$ there, and eq. (1.15) is easily satisfied without requiring that $\int_{-\infty}^{+\infty} \eta_0 dz$ vanish anywhere in the disk. However, eq. (3.62), presumes that Ω and j were approximately equal to their corresponding Keplerian values of Ω_0

and j_0. This then forced the vertically-integrated viscosity (and hence h) to be zero at the radius, r_+; ultimately leading to the calculated singularities in Ω, v_r and v_z.

In the final analysis, we arrive at the conclusion that our perturbative expansion in ϵ is not valid in the inner part of the disk, near $r = r_+$, if we use the simple analytical expression for $h(r)$ which appears in eq. (2.39). However, as they are written in terms of the disk surface, $h(r)$, our solutions for Ω_2, u_1, and v_2 in eqs. (2.52)-(2.56) are more general than they first appear. Numerical work (Kita & Kluźniak 1997) shows that the radius of convergence for our expansions can be extended well into the boundary layer ($r_+ \gtrsim r$) and all singularities completely disappear if only a more realistic (numerical) solution for h and $(d \ln h / d \ln r)$ is used. In any event, our solutions for the vertical structure are certainly valid in the outer regions of the disk for $r \gtrsim 2r_+$, where we are fully justified in assuming $\Omega \approx \Omega_k$, and hence in using eq. (3.62) to determine h.

4. The velocity vector field.

In this section we will examine the behavior of the horizontal and vertical components of the fluid velocity in the accretion disk. In particular, we will concern ourselves with the sign of v_r and v_z, so that we can determine the direction of the accretion flow. Note that we adopt here the convention that accompanied eq. (1.12), i.e. $\dot{M} > 0$ for accretion. Thus, if $v_r < 0$ the radial component of the flow is directed towards the central star. Likewise, $v_z < 0$ for $z > 0$ signifies flow towards the $z = 0$ midplane. Eqs. (2.53)-(2.57) for u_1 and v_2 directly give the unscaled velocity components as functions of r and z to lowest order in ϵ, i.e. $v_r(r, z) = \epsilon^2 u_1 \Omega_{k*} \tilde{R}$ and $v_z(r, z) = \epsilon^3 v_2 \Omega_{k*} \tilde{R}$.

4.1. The sign of v_r in the outer disk: outflow vs. inflow.

It is a result of our analysis, that at the surface of the accretion disk considered here, the fluid always flows in the general direction of the central object. Indeed, since $2 > (32/15)\Lambda\alpha^2$ for all possible α's in the range $0 \leq \alpha \leq 1$, then $v_r < 0$ for all points on the disk surface because the term in eq. (2.53) proportional to $(1 - z^2/h^2)$ vanishes at $z = \pm h$. However, near the midplane beyond a certain radius, there may or may not be outflow depending on the chosen value of the parameter of viscosity, α.

The radial velocity in the equatorial plane is:

$$v_r(r,0) = -\alpha\epsilon^2\Omega_{k*}\tilde{R}\left(\frac{h^2}{r^{5/2}}\right)\left[2\left(\frac{d\ln h}{d\ln r}\right) - \Lambda\left(1 + \frac{32}{15}\alpha^2\right)\right], \tag{4.63}$$

where $(d\ln h/d\ln r)$ can be obtained from eq. (2.44) and $\Omega_{k*}\tilde{R}$ provides the physical units. For small radii, $r \sim r_+$, evaluation of eq. (4.63) shows that the term involving $(d\ln h/d\ln r)$ dominates the bracketed expression and thus $v_r(r,0) < 0$, i.e. we have inflow. However, for large radii, $r \gg r_+$, we see that since $\lim_{r\to\infty}(d\ln h/d\ln r) = 1$, the sign of $v_r(r,0)$ depends ultimately on whether or not $2 \geq \Lambda(1 + 32\alpha^2/15)$.

If, for example, $\alpha = 0$, then Λ reduces to $11/5$ and the bracketed portion of eq. (4.63) is negative, so that $v_r(r,0) > 0$ for $r \gg r_+$; indicating the existence of outflow in the equatorial plane far from the central accretor[4]. On the other extreme, if $\alpha = 1$ then $\Lambda \approx 0.618$ and $\Lambda[1 + 32\alpha^2/15] \approx 1.94 < 2$ and so $v_r(r,0) < 0$ for $r \gg r_+$, signaling that the equatorial flow is directed inwards towards the central star for all radii. A more precise analysis of eq. (4.63) allows us to determine the critical value $\alpha_{cr} = \sqrt{15/32} \sim 0.685$ above which there is no backflow. This is a rather substantial

[4]To our knowledge, equatorial outflow in accretion disks was first discovered by Urpin (1984).

value more than ten times as large as the critical value estimated by Kley & Lin (1992).

We now analyze quantitatively where the direction of the flow changes sign when $\alpha < \alpha_{cr}$. To this end we denote the stagnation radius, r_{stag}, as the radius for which $v_r = 0$ in the equatorial plane. Eq. (4.63) with $\alpha < \alpha_{cr}$ allows us to calculate this stagnation radius as a function of α:

$$\frac{r_{stag}(\alpha)}{r_+} = \frac{\left[1 + 6\left(\Lambda(1 + \frac{32}{15}\alpha^2) - 2\right)\right]^2}{\left[6\left(\Lambda(1 + \frac{32}{15}\alpha^2) - 2\right)\right]^2}. \tag{4.64}$$

Observe that as $\alpha \to \alpha_{cr} = \sqrt{(15/32)}$, $\Lambda \to 1$ by eq. (2.54), and $r_{stag} \to \infty$, as expected. This behavior is clearly visible in Fig 3, where we have plotted $\log(r_{stag}/r_+)$ vs. α.

In the opposite limit $\alpha \to 0$, $r_{stag}/r_+ \to 121/36 \approx 3.36$. For $\alpha \leq 10^{-1}$, we see that $r_{stag} \approx 3.5 r_+$, this suggests that there is mass outflow in the midplane throughout most of the disk for realistic values of α.

Of course, for $\alpha < \alpha_{cr}$, the region of outflow is not restricted to the midplane $(z = 0)$. Indeed, inspection of eq. (2.53) shows that $v_r(r, z) \geq 0$ for a range of z above and below the equator for $r \geq r_{stag}$. We, therefore, define the "vertical flow surface," $z_{vert}(r, \alpha)$, as the surface on which $v_r = 0$, implying that the flow is moving vertically there and hence the name. Clearly, z_{vert} is well-defined for $r \geq r_{stag}$ and intersects the equatorial plane at $r = r_{stag}$. Thus we can expect there to be outflow in the disk for all points contained in the domain of $r > r_{stag}(\alpha)$ and $z < z_{vert}(r, \alpha)$, whenever $\alpha \leq \alpha_{cr}$. For $\alpha \geq \alpha_{cr}$ the surface of vertical flow disappears entirely.

Solving for z_{vert} via eq. (2.53) for u_1, we obtain

$$\left(\frac{z_{vert}(r, \alpha)}{h(r)}\right) = \sqrt{\left(1 + \frac{32}{15}\alpha^2\right) - \frac{2}{\Lambda}\left(\frac{d \ln h}{d \ln r}\right)}. \tag{4.65}$$

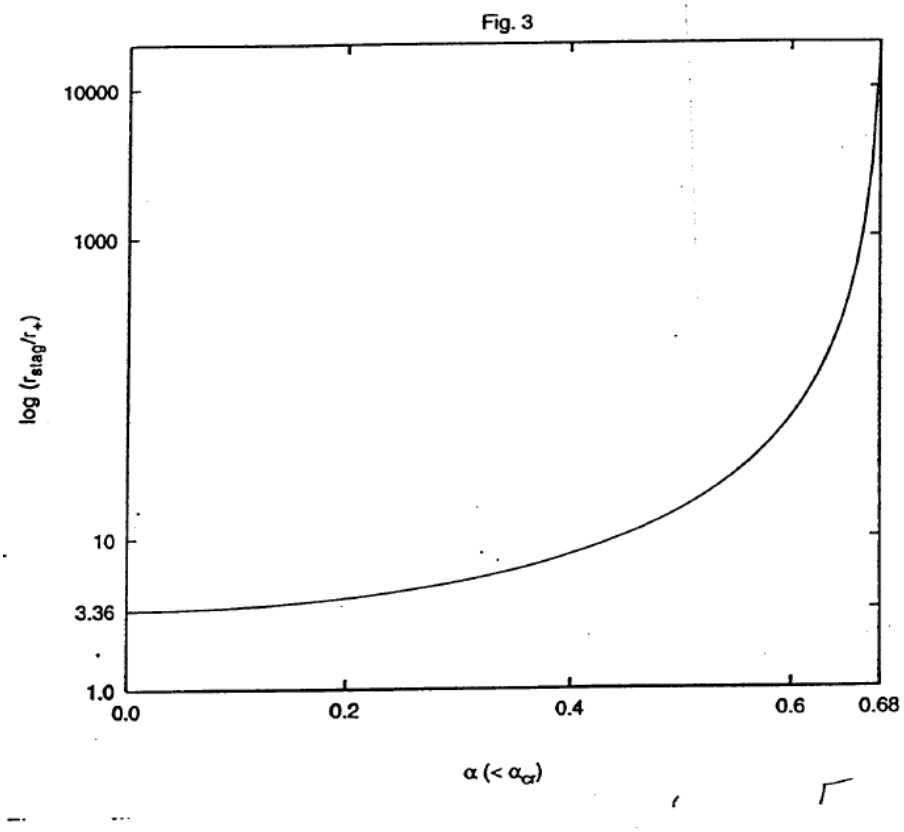

Fig. 3.— The stagnation radius vs. α. Observe that for $\alpha \leq 0.2$, $r_{stag} \leq 4.0 r_+$ (tending to $121/36 \approx 3.36$ for $\alpha = 0$), but diverges rapidly as $\alpha \to \alpha_{cr} = \sqrt{(15/32)} \approx 0.685$.

In Fig. 4, we show $\log(Z_{vert}/r_+)$ (solid curves) and $\log(H/r_+)$ (dashed curves) for two different values[5] of the parameter α: $\alpha = 0.1$ & $\alpha = 0.6$, where $Z_{vert} = \epsilon z_{vert}$ and $H = \epsilon h$. Observe that in Fig. 4, since $\alpha = 0.6$ is closer to $\alpha_{cr} \sim 0.685$, the outflow region, bounded from above by $z_{vert}(r, \alpha)$, is beginning to be strongly suppressed and does not even start in the equatorial plane until $r \gtrsim 60 r_+$. However, for $\alpha = 0.1$ in Fig. 4, the region of backflow is quite extensive and occupies nearly 30% of the disk

[5] H is also affected by the choice of α, since $h \propto (\dot{m}/\alpha)^{1/6}$.

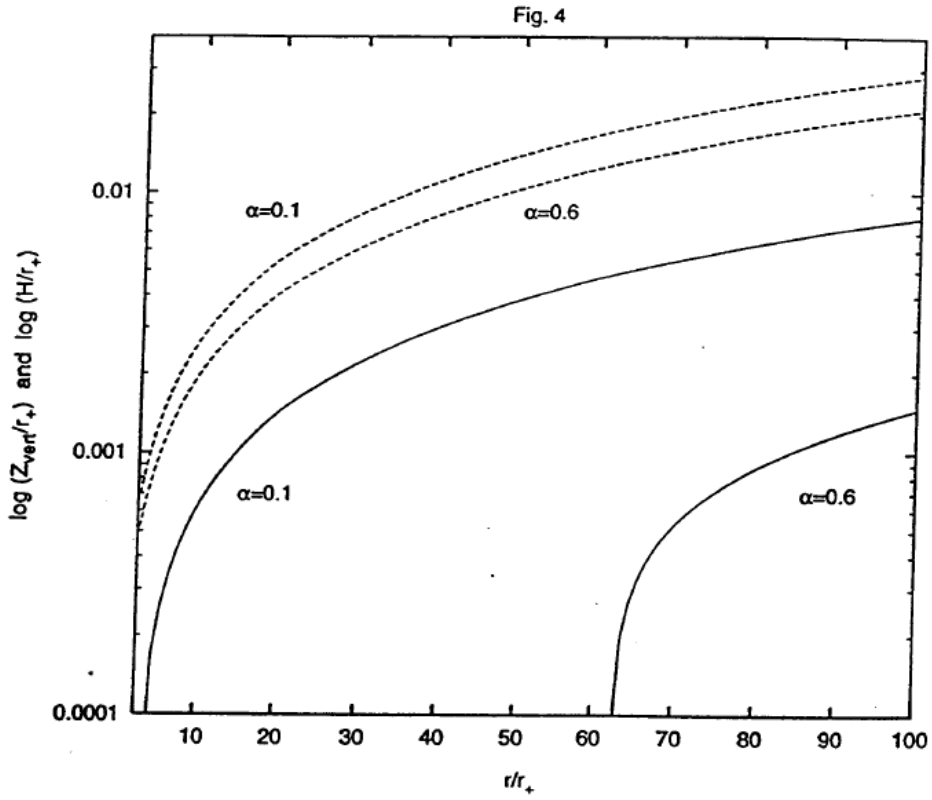

Fig. 4.— Logscale plot of $Z_{vert} = \epsilon z_{vert}$ (solid lines) and $H = \epsilon h$ (dashed lines) for $\alpha = 0.1$ and $\alpha = 0.6$, with $\epsilon = 0.01$ in both cases. Notice how much smaller the vertical flow surface is relative to the disk surface when $\alpha = 0.6$.

for $r \geq 10r_+$.

4.2. The sign of v_z and its impact on mass outflow.

We turn now our attention to the vertical velocity component, v_z. A study of eq. (2.56) reveals that $\pm v_z < 0$ for all points on the disk surface at $z = \pm h(r)$, respectively, signifying that the flow there is directed towards the equatorial plane. In addition, eq. (2.56) leads us to the conclusion that for $\alpha < \alpha_{cr}$, besides being zero for all radii in the ($z = 0$) midplane because of its odd parity, v_z also vanishes on a

new and different "horizontal flow surface", $z_{hor}(r,\alpha)$, on which the flow is directed horizontally.

We determine the following functional form for this surface:

$$\left(\frac{z_{hor}(r,\alpha)}{h(r)}\right) = \sqrt{\left(1+\frac{32\alpha^2}{15}\cdot\frac{d\ln h}{d\ln r}\right) - \frac{2}{\Lambda}\left(\frac{d\ln h}{d\ln r}\right)^2}. \tag{4.66}$$

Comparison of this result with eq. (4.65) reveals some definite similarities between the two flow surfaces, including the property that z_{hor} vanishes entirely in the limit $\alpha \to \alpha_{cr}$. We also observe that z_{hor}, the bounding surface across which v_z changes sign, is contained entirely within the vertical flow surface, z_{vert}, at which $v_r = 0$. Furthermore, as $r \to \infty$, z_{hor} asymptotically approaches z_{vert} from below for all values of α. Thus for $\alpha < \alpha_{cr}$, there is a nested volume contained within the domain of backflow ($v_r > 0$), within which the flow is directed away from the midplane,i.e. $v_z/z > 0$.

Figs. 5(a)-(b), illustrate this phenomenon for $\alpha = 0.1$ and $\alpha = 0.6$ respectively, where we have zoomed in to that fraction of the disk involved with outflow. Observe that at smaller radii, in both cases region A, the area within which $v_z/z > 0$, is much smaller than the corresponding region B within which $v_r > 0$; though their boundaries do converge to another at infinity, since $\lim_{r\to\infty}(d\ln h/d\ln r) \to 1$.

Eqs. (2.53)-(2.56), in conjunction with eqs. (4.65)-(4.66), also allow us to draw some rather interesting conclusions regarding the flow geometry in the outer disk. First, any material that enters region B must cross over into region A at some time in the future. To see this, note that v_z/z is still negative for all points between the vertical flow surface and the horizontal flow surface ($|z_{hor}| < |z| < |z_{vert}|$) and thus any fluid element in region B (where $v_r > 0$), given enough time, must eventually cross the inner horizontal flow surface, z_{hor}, and into region A. It is clear that some of the material in region C in Figs. 5(a)-(b) must not enter region B, instead a sizeable

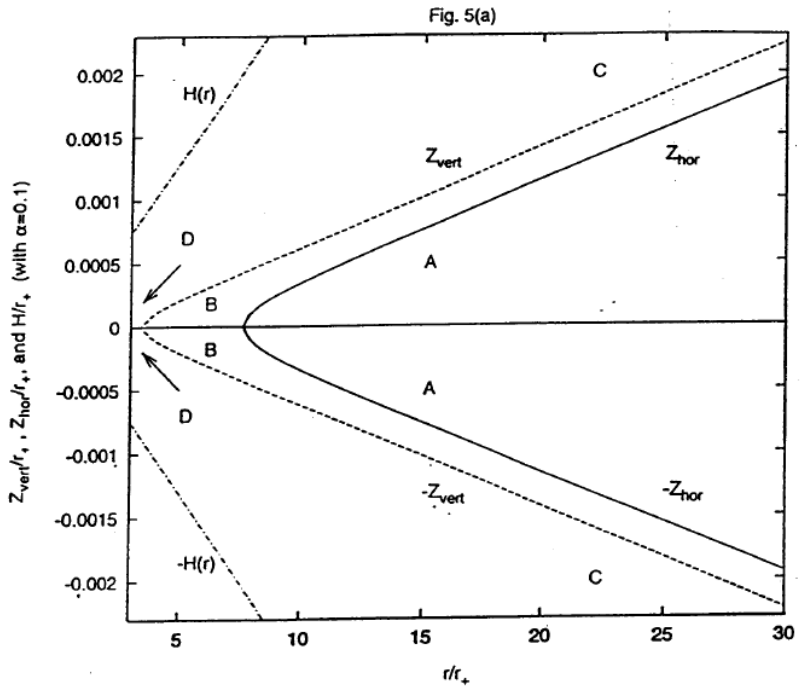

Fig. 5(a).— Plot of $Z_{vert} = \epsilon z_{vert}$ (solid lines), $Z_{hor} = \epsilon z_{hor}$ (dashed lines), and $H = \epsilon h$ (dot-dashed lines) for $\alpha = 0.1$ and $\epsilon = 0.01$. Region A represents the zone where $v_r > 0$ and $v_z/z > 0$, B labels the area where $v_r > 0$ and $v_z/z < 0$, and C marks the portion where $v_r < 0$ and $v_z < 0$. The arrows labeled D indicate the region where the fluid flows only towards the central object.

fraction of the flow that exists above z_{vert} must continue on ahead of the stagnation radius, into region D and onto the central star. This is, of course, the accreted flow that comprises $\dot{M}$.

To better visualize our previous remark, we call the reader's attention to Figs. 6(a)-(b), where we plot the direction of the velocity vector field, i.e. the unit vectors formed from the components v_r and v_z, in the outer disk for two different values of viscosity, both with $\alpha < \alpha_{cr}$. As a reference, we have also overlaid the vertical flow surface, z_{vert}. In Fig. 6(c), we show the directional flow pattern for the case of $\alpha > \alpha_{cr}$ (here $\alpha = 1$), and we now find that only inflow persists throughout the

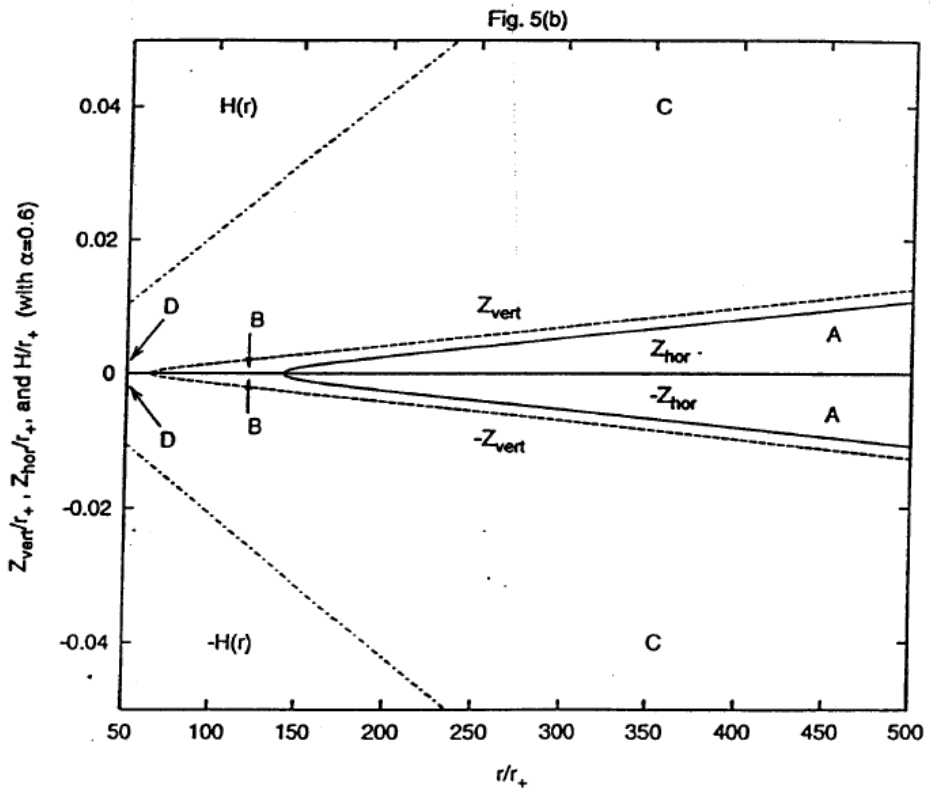

Fig. 5(b).— Same as Fig. 5(a) except now $\alpha = 0.6$. Note the change in scale and observe how much smaller the two flow surfaces are relative to the disk surface when $\alpha = 0.6$.

entire disk.

Finally, note that there are no cells of meridional circulation in the disk. In the region B flow is always directed towards the surface which bounds region A, while in the region A flow is always directed away from the equator. The circulating pattern of flow found by Kley & Lin (1992) close to the edges of their computational domain must be an artifact of the boundary conditions they imposed. In fact, calculation of the stream lines shows that material which enters region A can never intersect the $v_z = 0$ horizontal flow surface again, because $v_r > 0$ and $v_z \to 0$ there. Coupled with our original finding that any fluid which enters region B must also pass eventually into

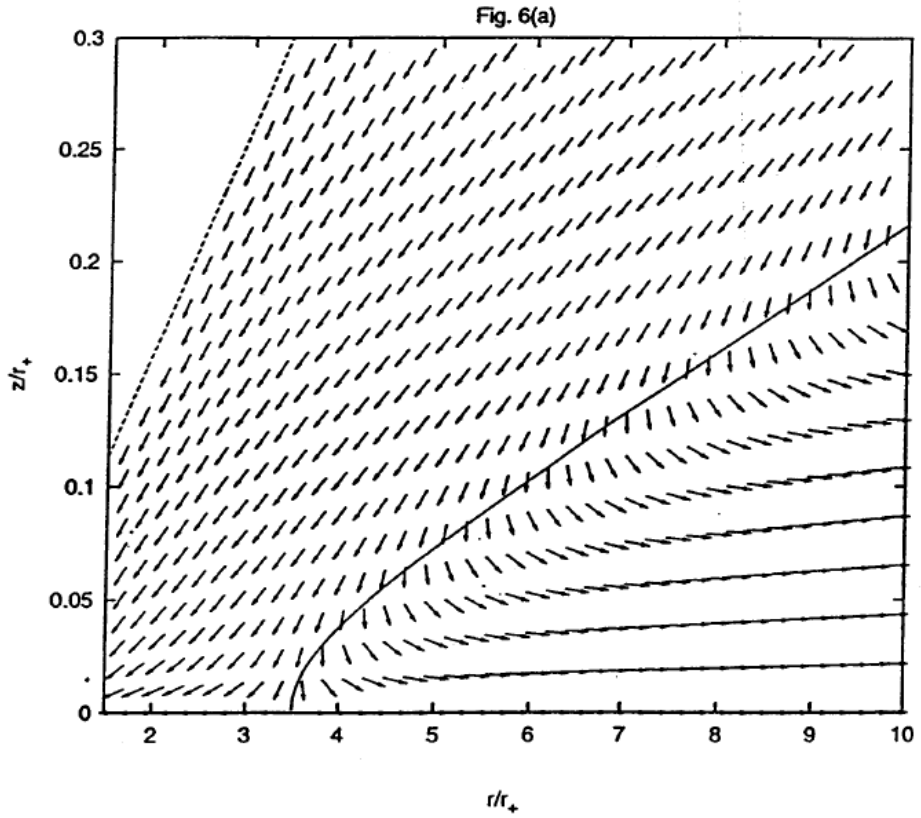

Fig. 6(a).— The unit velocity vector field, i.e. $(\vec{v_r}/|v_r|,\vec{v_z}/|v_z|)$ for $\epsilon = 0.1$ and $\alpha = 0.1$. The dashed curve represents the disk surface and the solid curve the vertical flow surface where $v_r = 0$.

region A, this implies that material once in the backflow region B can never return to the inflow portion C of the accretion disk. Therefore, if $\alpha < \alpha_{cr}$, the backflow must continue all the way out to "infinity," where the disk terminates. All of this can be easily verified by looking at Figs. 6(a)-(b).

4.3. The mass fraction of outflow relative to inflow.

The last question that we address relates to the backflow. What is the mass outflow rate in comparison to the $\dot{M}$ accreted by the star? It is clear that the answer

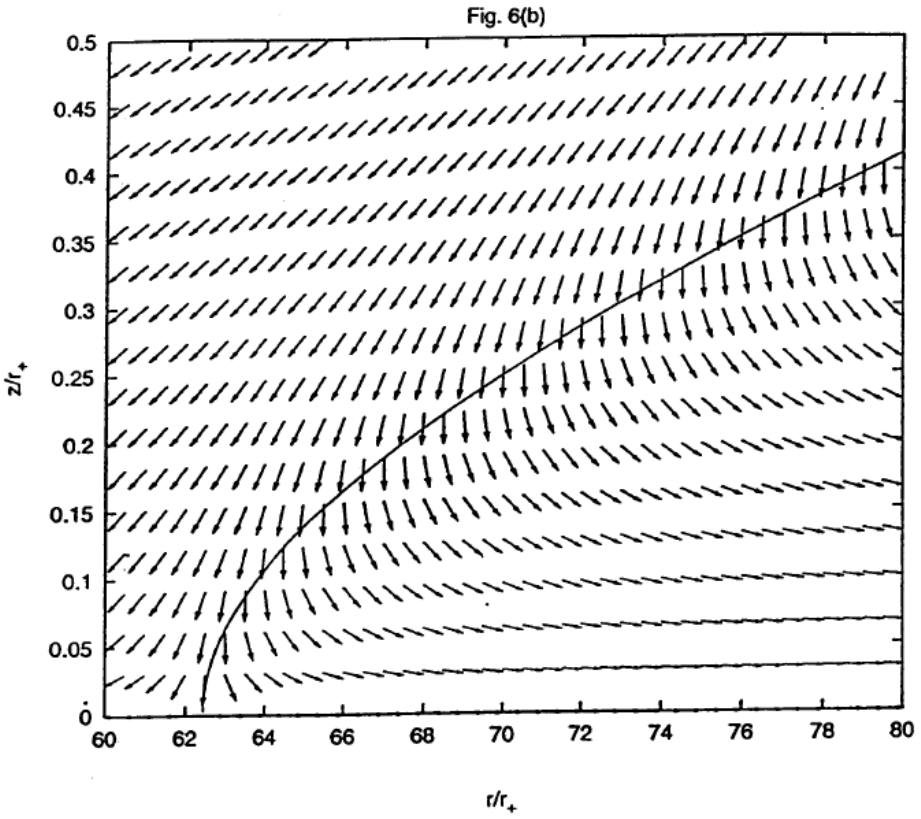

Fig. 6(b).— Same as Fig. 6(a) except now $\alpha = 0.6$. Note that because the outflow region has been greatly reduced and pushed out to $r \geq 62.5r_+$, we have zoomed in to the equatorial region near the stagnation radius.

to this question must depend on the parameter α, since we know that there is no backflow for $\alpha \geq \alpha_{cr} \sim 0.685$. For this reason we now define $\Gamma(r, \alpha)$ to be the ratio of the mass rate flowing outwards through a cylinder of radius $r > r_{stag}$ to the net mass accretion rate, $\dot{M}$.

To evaluate the functional form of $\Gamma(r, \alpha)$, we simply integrate the radial mass flux, ρv_r, over the surface of a cylinder with height $2z_{vert}$ centered on the midplane.

$$\Gamma(r,\alpha) = \left| \frac{4\pi r \int_0^{z_{vert}(r,\alpha)} \rho_0 u_1 dz}{4\pi r \int_0^{h(r)} \rho_0 u_1 dz} \right| = \frac{1}{\dot{m}} \left| 2r \int_0^{z_{vert}(r,\alpha)} \rho_0 u_1 dz \right|, \tag{4.67}$$

where $\dot{m}$ is the scaled mass accretion rate defined in eq. (2.34).

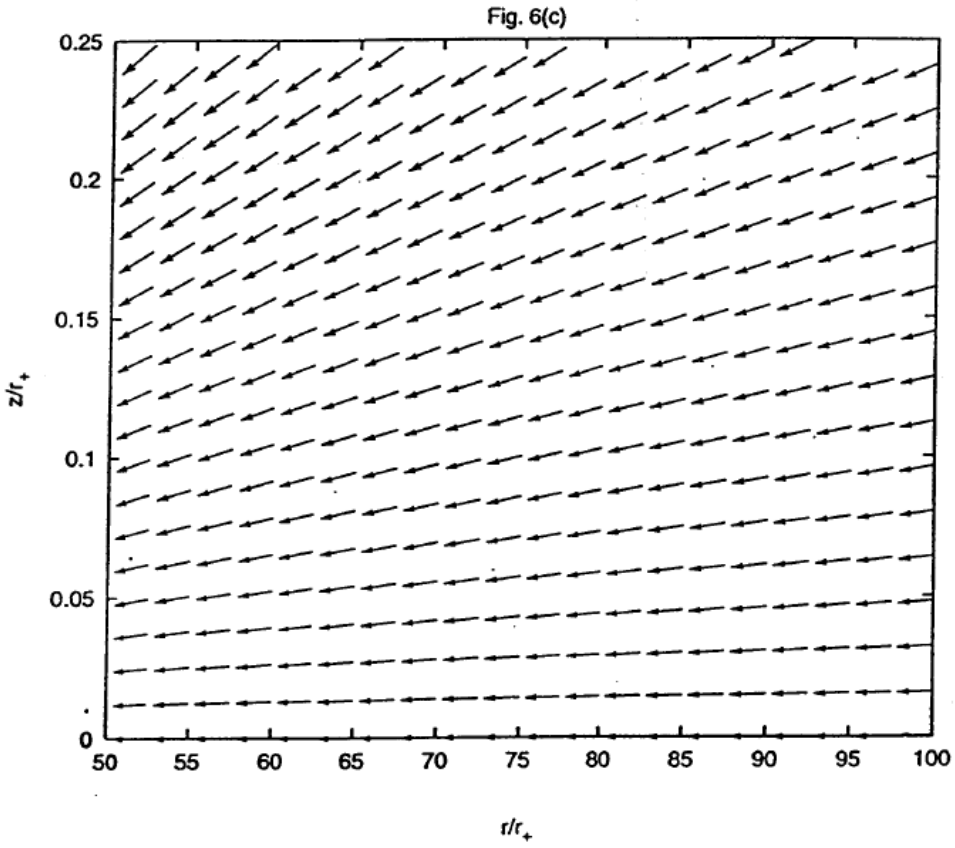

Fig. 6(c).— Same as Figs. 6(a)-(b) except now $\alpha = 1.0$. There is no longer any outflow in the disk as $\alpha > \alpha_{cr} \approx 0.685$.

Using eq. (4.65) for $z_{vert}(r, \alpha)$, eq. (2.31) for ρ_0, and eq. (2.53) for $u_1(r, z)$ we find that the mass outflow fraction is

$$\Gamma(r, \alpha) = \left(\frac{2\alpha\Lambda}{5\sqrt{5}\dot{m}}\right)\left(\frac{h}{r}\right)^6 \left[G_1(\gamma^*) + \left((\gamma^*)^2 - 1\right) G_2(\gamma^*)\right] \tag{4.68}$$

where $\gamma^* = \gamma^*(r, \alpha) = z_{vert}/h$ and G_1 and G_2 are rather complicated functions of γ^* given by:

$$G_1(\gamma^*) = \int_0^{\gamma^*} \left(1 - \frac{z^2}{h^2}\right)^{5/2} \frac{dz}{h} = \frac{5}{16}\sin^{-1}(\gamma^*) + \frac{5}{16}\gamma^* \left(\sqrt{1 - (\gamma^*)^2}\right) + \frac{5}{24}\gamma^* \left(\sqrt{1 - (\gamma^*)^2}\right)^3 + \frac{\gamma^*}{6}\left(\sqrt{1 - (\gamma^*)^2}\right)^5, \tag{4.69}$$

$$G_2(\gamma^*) = \int_0^{\gamma^*} \left(1 - \frac{z^2}{h^2}\right)^{3/2} \frac{dz}{h} = \frac{3}{8}\sin^{-1}(\gamma^*) + \frac{3}{8}\gamma^* \left(\sqrt{1-(\gamma^*)^2}\right) + \frac{1}{4}\gamma^* \left(\sqrt{1-(\gamma^*)^2}\right)^3 . \tag{4.70}$$

The limit $\Gamma_\infty(\alpha) = \lim_{r\to\infty} \Gamma(r,\alpha)$ is of particular interest, as it represents the ratio of the net outflow to net inflow in the disk.

Analysis of eqs. (4.68)-(4.70) provides us with the following form for Γ_∞:

$$\Gamma_\infty(\alpha) = \frac{32\Lambda}{\pi}\left[G_1(\gamma^*_\infty) + \left((\gamma^*_\infty)^2 - 1\right) G_2(\gamma^*_\infty)\right], \tag{4.71}$$

where the quantity γ^*_∞ is well defined only for $\alpha < \alpha_{cr}$ and given by

$$\gamma^*_\infty = \lim_{r\to\infty} \gamma_*(r,\alpha) = \sqrt{1 + \frac{32}{15}\alpha^2 - \frac{2}{\Lambda}}. \tag{4.72}$$

The resultant dependence on α for the mass outflow fraction as $r \to \infty$ is plotted in Fig. 7. We see that $\Gamma_\infty(\alpha)$ tends smoothly to zero as $\alpha \to \alpha_{cr}$. However, for a wide range of α, the fraction of the mass flow that is contained in the outflow region, near the midplane is quite significant: $\Gamma_\infty(\alpha) \sim 0.4$ for $0 \le \alpha \lesssim 0.1$ and $0.1 < \Gamma_\infty(\alpha) \lesssim 0.35$ for $0.1 < \alpha < 0.5$. Thus, for $\alpha \le 0.1$, the total mass rate, $\dot{M}_{tot} = \dot{M}_{out} + \dot{M}$, being fed into the disk at the outer edge is $\approx 1.4\dot{M}$.

All in all, we are led to the startling conclusion (Urpin 1984) that, for small values of α, there is backflow in the disk transporting fluid outwards to the outer boundary of the accretion disk. This should have serious repercussions for mass transfer at the outer edge of the disk.

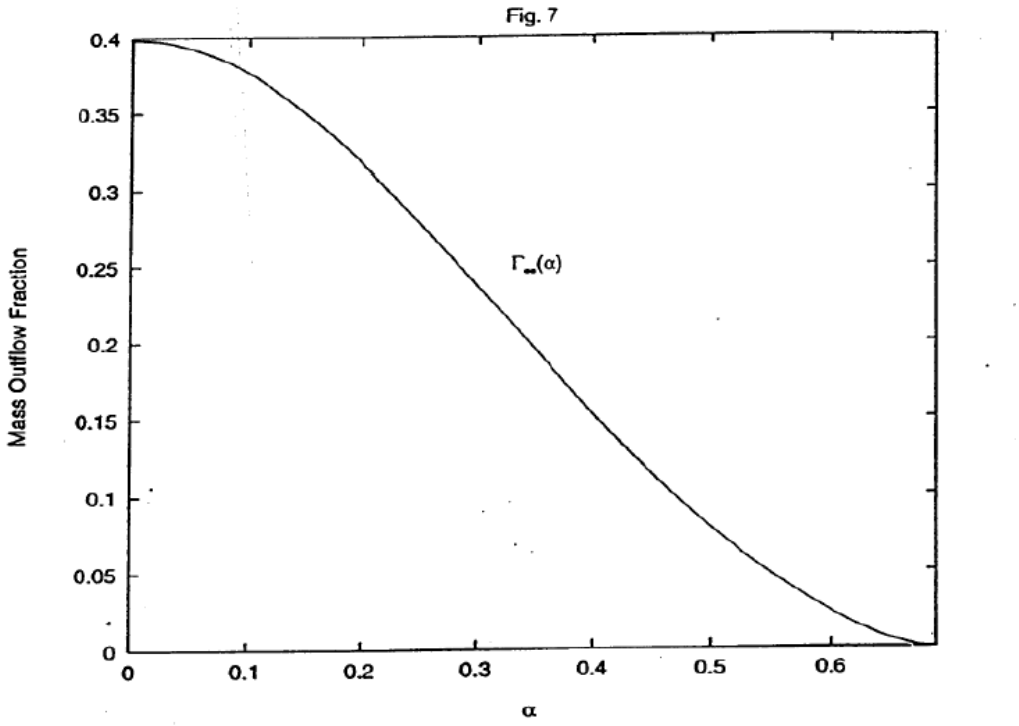

Fig. 7.— The ratio of the mass flow rate of material moving outwards (through a cylinder with $r = \infty$) to the net accreted mass flow rate, $\dot{M}$, vs. α. Observe that $\Gamma_\infty(\alpha)$ vanishes as $\alpha \to \alpha_{cr} \approx 0.685$, but is about 40% for $\alpha < 0.1$.

6. Final remarks.

By performing a systematic expansion (pioneered by Regev 1983) of the disk equations of motion we were able to find a closed solution for the velocity field and the disk structure, valid everywhere outside, say, 1.1 times the zero torque radius. We showed how, for all but very large values of viscosity, the accretion flow turns around and feeds a backflow (first discovered by Urpin in 1984) in the equatorial plane of the disk. This backflow has now also been seen in a number of numerical simulations and must

be considered a general feature of accretion in a geometrically thin disk, and possibly also in quasi-spherical flows.

We note, that if the flow discussed here were advective, some of the gravitational energy released by the flow close to the central gravitating body would have been carried by the flow to larger radii before it is radiated. An urgent topic of investigation should be whether solutions with backflows, similar to the one presented here, may be present in an advection dominated flow. Should such solutions exist, conclusions (e.g. Narayan 1996) that the apparent deficit of emission in the inner region of accretion disks of some X-ray "novae" necessarily implies the presence of a space-time horizon would have to be treated with caution.

REFERENCES

Frank, J., King, A.R. & Raine, D.J. 1992, Accretion Power in Astrophysics, Cambridge University Press.

Hōshi, R. 1977, Prog. Theor. Phys. 58, 1191.

Igumenshchev, I.V., Chen, X. & Abramowicz, M.A. 1995, MNRAS 278, 236–250.

Kita, D. B. 1995, Ph. D. Thesis, University of Wisconsin-Madison.

Kita, D. B. & Kluźniak W. 1997, in preparation.

Kluźniak W. 1987, Ph. D. Thesis, Stanford University.

Kley, W. & Lin, D.N.C. 1992, ApJ 397, 600–612.

Landau, L.D. & Lifshitz, E.M. 1959, Fluid Mechanics, Pergamon Press.

Monin, A.S. & Yaglom, A.M. 1965, Statistical Fluid Mechanics: 1, Nauka: Moscow [MIT Press, 1971].

Narayan, R. 1996, ApJ 462, 136–141.

Narayan, R. & Yi 1995, I. ApJ 444, 231–243.

Paczyński 1991, ApJ 370, 597–603.

Prendergast, K.H. & Burbidge, G.R. 1968, ApJ 151, L83–L88.

Regev, O. 1983, AA 126, 146–151.

Różyczka, M., Bodenheimer, P. & Bell, K.R. 1994, ApJ 423, 736–747.

Shakura, N.I. & Sunyaev, R.A. 1973, AA 24, 337–355.

Tassoul, J.L. 1978, Theory of Rotating Stars, Princeton University Press.

Urpin, V.A. 1984, Astron. Zh. 61, 84–90 [Sov. Astron. 28, 50–53].

Urpin, V.A. 1984b, Astrophys. Sp. Sci. 90, 79.